

University of Dayton

eCommons

Electrical and Computer Engineering Faculty
Publications

Department of Electrical and Computer
Engineering

3-11-2021

The Physics of Fire by Friction

Bradley D. Duncan

Follow this and additional works at: https://ecommons.udayton.edu/ece_fac_pub



Part of the [Physics Commons](#)

The Physics of Fire by Friction

by Bradley D. Duncan, Ph.D.
January, 2021

1. Introduction

I made my first bow drill kit, and lit my first friction fire, at Ransburg Scout Reservation in June, 2016. I was there with my Boy Scout troop (Troop 516, Centerville, OH) for our annual summer camp adventure. Ransburg is, of course, the modern day home of Firecrafter [1]. Our troop has a rich, decade's long history of active participation in the Firecrafter program and I'd been watching our scouts pursue the various rank requirements with increasing interest since I joined the troop as an assistant Scoutmaster in early 2014. I was especially intrigued by the almost mystical way our Firecrafters and Firecrafter candidates could conjure smoke and fire by merely "rubbing sticks together."

My obvious interest eventually led to me being invited to join the organization as an adult member of the Firecrafter Alumni Association. Those nominated to become Firecrafters as adults are actually not required to submit to any of the grueling ordeals experienced by youth candidates. Nevertheless, I felt duty and honor bound to try and master all the requirements of the three Scout ranks; Camper, Woodsman and Firecrafter. My fascination with the idea of making fire by friction made this quest especially exciting! Four and a half years later I am still fascinated by it all. Studying fire by friction and other primitive firemaking methods has actually become quite an entertaining little hobby of mine. My wife and kids think I'm nuts, but becoming a Firecrafter has been one of the most rewarding and fun things I've ever done. I love it!

I am also an engineer with a Ph.D. in Electrical Engineering (VA Tech, vintage of 1991). I've spent most of the past 30 years as a Professor and researcher at the University of Dayton, Dayton, OH, with the majority of my scientific pursuits focusing on the areas of fiber optics, optical remote sensing and laser radar. This, of course, leaves me almost completely unqualified to attempt to write an article on the physics of fire by friction, but I decided to give it a try anyway. It's difficult to pursue a meaningful research career without crossing a few disciplinary boundaries from time to time. If nothing else, I'm pretty good with math. With a little patient reflection, I thought, maybe I can pull together enough fragments from my long ago studies of mechanics, dynamics and thermodynamics to pull it off. We'll see. In true Firecrafter fashion, I will certainly *do my best!*, but you my dear reader must ultimately be the judge. As I tell my graduate students, it's the peer review process that separates the discovery of authentic new knowledge from mere conjecture and opinion.

In what follows I will attempt to produce a rigorous, macroscopic, time averaged model of the process of creating fire by friction – up to the point of initial ember formation. I will employ reasonable, practical approximations with the goal of developing mathematical results that are experimentally

verifiable. Although force, velocity, pressure and the like are actually vector quantities, due to the symmetry of the problem I will perform a scalar analysis only. Also, to simplify the analysis I will assume that the assortment of variables we will encounter are independent. Mostly this assumption is valid, though on occasion I will point out where the assumption is, or may be weak. I will also occasionally point out where further research and analysis may be of interest to pursue.

There are, of course, a variety of methods for creating fire by friction. This article will focus exclusively on fire drills with solid rotating spindles. The initial analysis will focus on the bow drill, though near the end I'll describe some modifications that will make the models I'll develop appropriate for the pump drill as well. I have made no attempt to model the fire thong, fire saw, fire plow or any other method of fire by friction.

What about hand drills, you might ask? Well, hand drill methods commonly employ spindles made from wild flower stalks that have hollow or pith filled cores. To a first order, then, hand drill fire by friction can be described by the results developed within, if we agree to subtract off the effects of a hypothetical spindle with a diameter equal to that of the pith/hollow core, where little if any friction heat is developed. It's actually a bit more complicated than that and I'd be happy to share my notes on the subject with anyone who might be interested. Lastly, my discussions throughout will tacitly assume a reader who knows at least the fundamentals of fire by friction using a bow drill kit. If not, it's probably best to stop reading and go practice. This article will serve as a lousy tutorial for practical firemaking, though an experienced firemaker may gain some insights for further refining their craft.

2. Kinetic Friction

Any article on fire by friction must start with at least a brief discussion of friction itself. Simply, friction is a resistive force between two surfaces that are sliding, or trying to slide, across one another. As shown in Figure 1 for the simple case of horizontal linear motion, friction always opposes motion.

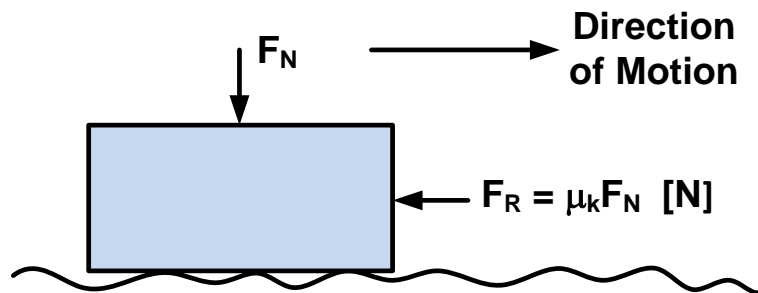


Figure 1: The friction force F_R is proportional to the total normal force F_N , and always opposes motion.

There are two main types of friction, static and kinetic. Static friction operates between two surfaces that aren't yet moving relative to one another, while kinetic friction acts between objects in motion. As shown in Figure 1, assuming the rectangular object is currently in motion the kinetic friction force F_R is directly proportional to the total normal force F_N acting perpendicular to the interaction surface. Simply put, $F_R = \mu_k F_N$ [N], where μ_k is the coefficient of kinetic friction and the unit of force is the Newton (See Appendix A) [2].

When two surfaces move with respect to one another the kinetic frictional force is almost constant over a wide range of low speeds. The coefficient of kinetic friction μ_k is also typically less than the coefficient of static friction μ_s , reflecting the common experience that it is easier to keep something in motion across another surface than it is to start it in motion from rest [3]. For this article I will limit my discussion exclusively to kinetic friction. All references hereafter to “coefficient of friction” will therefore imply “kinetic coefficient of friction” without ambiguity.

The coefficient of friction is a unitless quantity less than unity that depends on a variety of variables including the material(s) under consideration, surface condition, lubrication, etc. For dry wood moving across dry wood, of interest to us, the coefficient of kinetic friction varies between $0.17 \leq \mu_k \leq 0.48$, with most references putting μ_k in the range of 0.2-0.3 [e.g., 3, 4, 5]. For oak-on-oak with perpendicular grain, $\mu_k \approx 0.32$ [3]. Determining the coefficient of kinetic friction for a variety of charred woods commonly used in fire by friction would make a very interesting project for further research. In the absence of better data to work from, though, I’ll assume a mid-range value of $\mu_k = 0.25$ in order to allow me to perform some computations later on. This is probably the weakest assumption I will make, yet it will yield surprisingly good results later on and so may be reasonable.

3. Net Moment Due to Friction

The moment M of a force F is a measure of its tendency to cause a body to rotate, or resist rotation, about an axis. Moment and torque (possibly a more familiar term) are largely synonymous and increase in direct proportion to the lever arm length d . As shown in Figure 2, below, moment is simply $M = Fd$ [N-m].

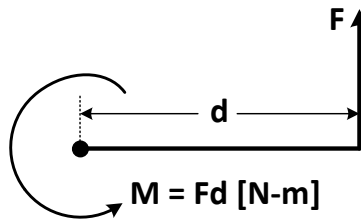


Figure 2: A simple moment diagram.

In the case of fire by friction employing a solid spindle rotating against a stationary fireboard, we must first distribute the normal force F_N across the interaction surface between the spindle and fireboard. I will assume the interface to be spherical in shape – a very good assumption that I’ll demonstrate later on. To determine the net, or aggregate moment due to friction opposing spindle motion, we must then employ calculus to integrate (i.e., sum up) the incremental moments across the entire contact area. In our case, this will require a two dimensional surface integration in spherical coordinates. Please hang on if this calculus is unfamiliar to you. It will be over soon enough.

The geometry of the problem is shown in Figure 3. The spherical coordinate variables are (r, θ, ϕ) and the figure is drawn to show a right handed coordinate system. The center of curvature of the spherical interface is designated by C . The polar angle ϕ is then taken with respect to the central axis, r is the radial distance from the center of curvature and the azimuth angle θ is defined in a plane perpendicular to the total normal force F_N (which includes the weight of the spindle itself, plus all applied external forces). The radius of curvature of the spherical interface is R_c and the maximum polar angle at the edge of the interaction area is ϕ_o . The radius of the spindle is then $R_o = R_c \sin(\phi_o)$, while the depth of the fireboard divot is h_o . Finally, the pressure P results from distributing F_N across

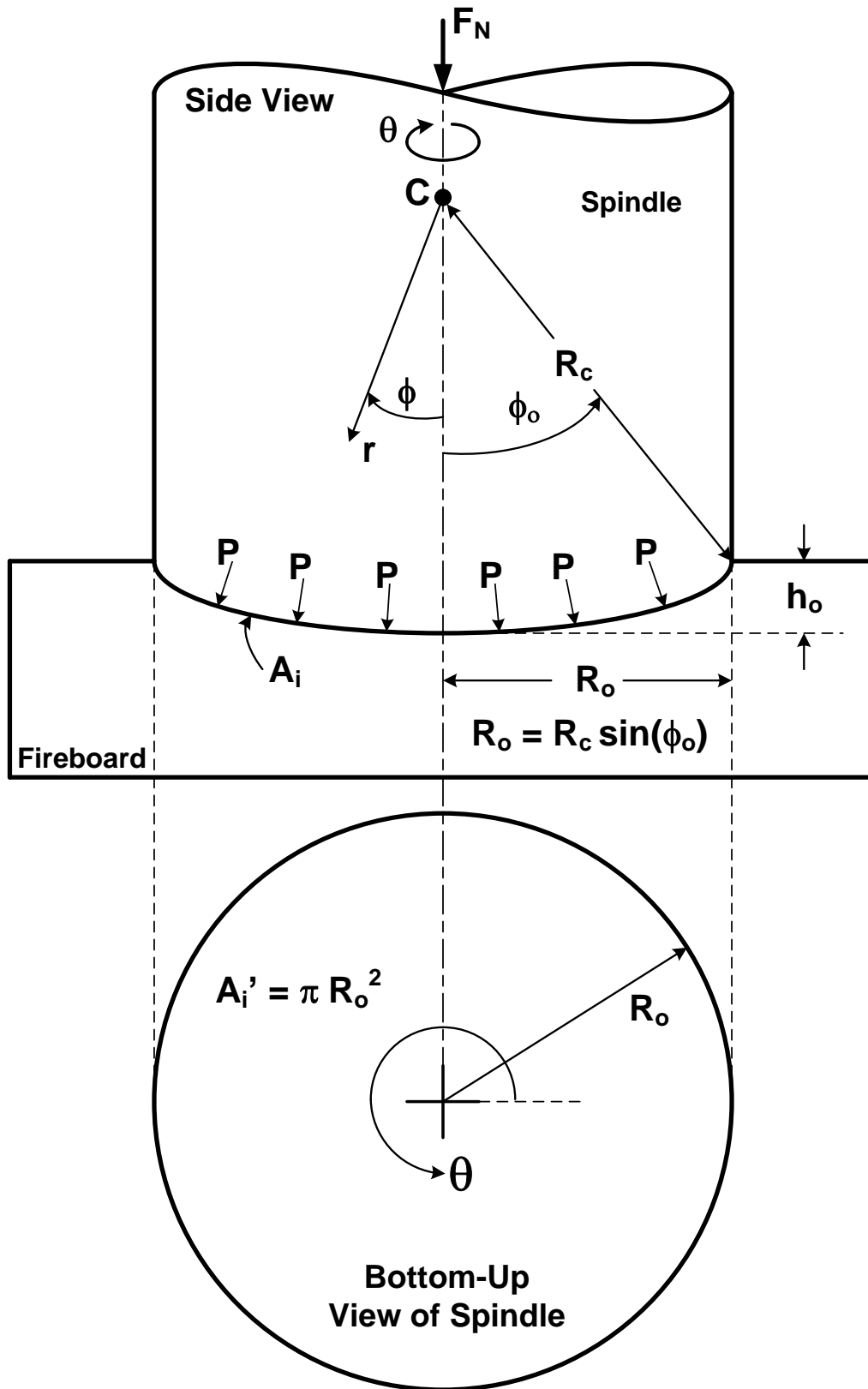


Figure 3: Spherical geometry of the spindle-fireboard interface.

the interaction area, A_i is the area of the spherical interface, and $A_i' = \pi R_o^2$ is the area of the spherical interface projected onto a plane perpendicular to the central axis.

With the additional assumptions that the spindle and fireboard are inelastic (i.e., there is no deformation of either due to the applied normal force F_N) and that there is negligible clearance at the spindle-fireboard interface (i.e., their curved shapes are perfectly matched after initial burn-in), then it can be shown that the pressure P across the interface is uniform and expressed by [6]

$$P = \frac{F_N}{A_i'} = \frac{F_N}{\pi R_o^2} \text{ [N/m}^2\text{]}. \quad (1)$$

The calculation of the net friction induced moment M_s at the spherical interface now proceeds in a manner inspired by the calculation of net moment in disc brake systems [7]. To begin we have

$$M_s = \int_0^{2\pi} \int_0^{\phi_o} f(\theta, \phi) dA \text{ [N-m]}, \quad (2)$$

where in spherical coordinates the differential area $dA = R_c^2 \sin(\phi) d\theta d\phi$ [m²], and the incremental moment per unit area $f(\theta, \phi)$ is given by

$$f(\theta, \phi) = \mu_k P R_c \sin(\phi) \text{ [N/m]}. \quad (3)$$

Notice that since equation (2) represents an area integral, the integrand $f(\theta, \phi)$ must have units of [N/m] in order for M_s to have the proper units of [N-m]. The expression in equation (3) ensures this result since pressure P (force per unit area) has units of [N/m²] and the moment arm $R_c \sin(\phi)$ has units of [m]. Also notice that the incremental moment of equation (3) is uniform with respect to the azimuth angle θ . Proceeding with the integration and simplifying the result we find that

$$\begin{aligned} M_s &= 2\pi \mu_k \frac{F_N}{\pi R_o^2} \int_0^{\phi_o} R_c^3 \sin^2(\phi) d\phi \\ M_s &= \mu_k F_N R_o \left(\frac{R_c}{R_o}\right)^3 \left[\phi_o - \frac{\sin(2\phi_o)}{2}\right] \\ M_s &= \mu_k F_N R_o \left(\frac{R_c}{R_o}\right)^3 [\phi_o - \sin(\phi_o)\cos(\phi_o)] \\ M_s &= \mu_k F_N R_o \left(\frac{R_c}{R_o}\right)^3 \left[\sin^{-1}\left(\frac{R_o}{R_c}\right) - \frac{R_o}{R_c} \cos\left(\sin^{-1}\left(\frac{R_o}{R_c}\right)\right)\right] \\ M_s &= \mu_k F_N R_o \left[\left(\frac{R_c}{R_o}\right)^3 \sin^{-1}\left(\frac{R_o}{R_c}\right) - \left(\frac{R_c}{R_o}\right)^2 \sqrt{1 - \left(\frac{R_o}{R_c}\right)^2}\right] \\ M_s &= \frac{2}{3} \mu_k F_N R_o S_M(\rho) \text{ [N-m]}, \quad (4) \end{aligned}$$

where $\rho = (R_c/R_o) \geq 1$, and $S_M(\rho)$ is a unitless spherical moment factor we will examine shortly. In arriving at equation (4) I also employed the following trigonometric identities:

$$\sin(2x) = 2 \sin(x) \cos(x) \quad \text{and} \quad \cos(\sin^{-1}(x)) = \sqrt{1 - x^2}.$$

To examine the spherical moment factor in more detail let's first write it out explicitly as

$$S_M(\rho) = \frac{3}{2} \left[\rho^3 \sin^{-1} \left(\frac{1}{\rho} \right) - \rho^2 \sqrt{1 - \left(\frac{1}{\rho} \right)^2} \right]. \quad (5)$$

Despite the apparent complexity of $S_M(\rho)$ it is actually very well behaved, as demonstrated in Figure (4). For large ρ , indicating a nearly planar spindle-fireboard interface, the spherical moment factor approaches unity, as confirmed in [7]. By contrast, for a hemispherical interface for which $R_c = R_o$, or $\rho=1$, we find that $S_M(\rho) = 1.5(\pi/2) = 3\pi/4 = \sim 2.356$.

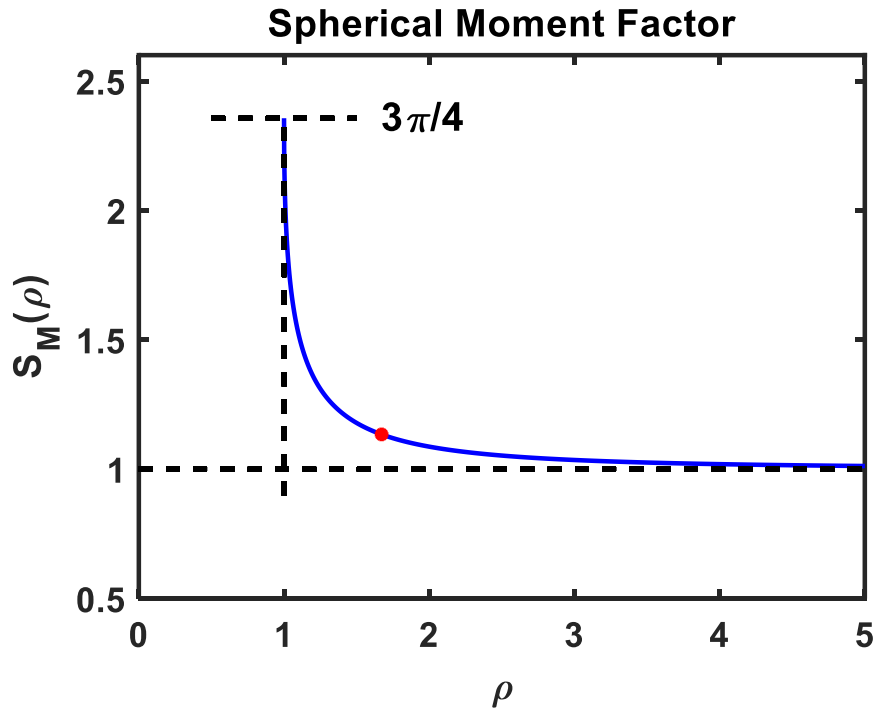


Figure 4: The spherical moment factor approaches unity for a nearly flat spindle-fireboard interface surface, and approaches $3\pi/4$ as the interface becomes increasingly hemispherical. The red dot represents the value realized in the experiment discussed later in Section 6.

Since $S_M(\rho)$ is a purely geometric shape factor, one early conclusion we can draw from examination of equations (4) and (5) is that highly hemispherical spindles and mating fireboard divots will generally be to our advantage in making embers more quickly. That is, all things being equal we will soon see the heat energy we can generate per unit time increases in direct proportion to the net moment due to friction and that, somewhat surprisingly, is directly influenced by spindle shape. Ah, the beauty of scientific discovery!

The astute reader may now be wondering about the notch we typically cut into our fireboards after burning in a new divot. The notch is required in order for charcoal dust to collect as the spindle and divot heat up while we bow. The notch is also required in order for friction heat to be conductively transferred to the dust, allowing ember ignition to take place. So, would accounting for the notch affect the calculations above? As it turns out, no. Nominally, if we remove the area of the notch from the fireboard, the normal force F_N is distributed over a smaller area, meaning the pressure P increases. This increased pressure is then integrated over a correspondingly smaller area in the integral of equation (2). The effects then cancel and the results of this section would be unchanged. If you are interested, I demonstrate this more explicitly in Appendix B.

4. Rotational Work, Energy and Power

For a force F acting linearly, the work W done by F is the energy expended in moving an object a distance d . Expressed mathematically, $W = Fd$ [N-m]. Note, though, that since work is an expression of expended energy it must have units of Joules, or [J]. Indeed 1 [N-m] of work is equal to 1 [J] of energy. Similarly, for moments and torques (i.e., rotational forces), energy is expended when the moment or torque acts on, or rotates, an object through an angle θ , expressed in radians [rad]. Mathematically, for a moment M , work $W = M\theta$ [N-m] or [J] [8, 9, 10, 11].

Note that in Section 3 we calculated the net moment due to friction and found that it had units of [N-m]. Although net moment appears to have units of energy, it isn't appropriate for us to express moments in units of [J] until they are allowed to act over some angle θ . Note also that this implies the unitless nature of angle θ . If this is surprising to you, please see Appendix C for a discussion of the unitless nature of angular measurements such as radians [rad].

For the net moment due to friction expressed in equation (4), the work W_F done when a spindle is made to rotate through an angle θ can be written simply as

$$W_F = \frac{2}{3} \mu_k F_N R_o S_M(\rho) \theta \text{ [J]} . \quad (6)$$

Keep in mind now that as we drive our bow drills the spindles periodically rotate clockwise (CW), then counterclockwise (CCW). These periodic changes in rotation direction don't matter at all, though, since friction always opposes motion, or in this case, rotation. Therefore θ in equation (6) represents the *cumulative* angular rotation, both CW and CCW, through which the spindle is made to rotate as we bow.

Similar to work, power is energy expended per unit of time. Power has units of [J/s] = [Watts] or [W]. The frictional power, or energy released per unit of time, can then be found by simply replacing the cumulative angle of rotation θ in equation (6) with the spindle's time averaged rotational angular velocity ω according to

$$P_F = \frac{2}{3} \mu_k F_N R_o S_M(\rho) \omega \text{ [W]} . \quad (7)$$

However, it is probably more useful and interesting to express P_F in terms of the average speed V_B at which we manipulate our bows. This conversion is aided by examining the geometry of Figure 5, where the outer surface of our spindle is assumed to be moving at speed V_B . By simple inspection we see that

$$V_B = \frac{S}{\Delta t} = \frac{R_o \theta}{\Delta t} = R_o \omega , \quad (8)$$

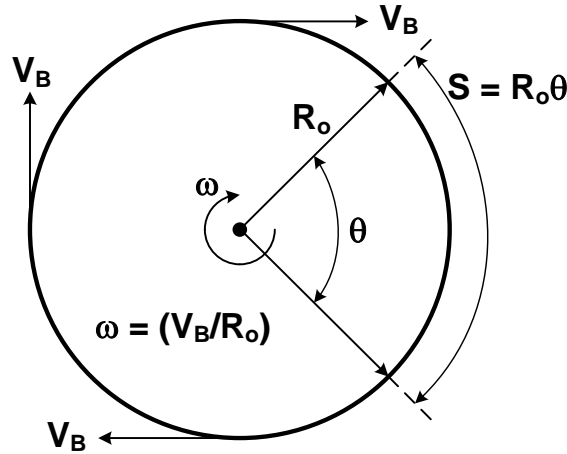


Figure 5: Linear bow speed V_B , acting on a spindle with radius R_o , causes the spindle to rotate with angular velocity $\omega = V_B/R_o$ [1/s].

where S is the arc length subtended by angle θ , and Δt is the time it takes for the spindle to rotate by angle θ . Solving equation (8) for ω and inserting the result into equation (7) then yields

$$P_F = \frac{2}{3} \mu_k F_N S_M(\rho) V_B \text{ [W]}. \quad (9)$$

Once again, keep in mind that V_B in equation (9) is the *average* bow speed, taking into account the stopping, starting, accelerations, decelerations and assorted direction changes that take place as we bow. It will be less than the peak bow speed at mid-stroke. This will perhaps become a bit clearer in the experimental section below.

Also notice, somewhat surprisingly, that equation (9) is independent of spindle radius R_o . This is because angular velocity ω is inversely related to spindle radius when substituting equation (8) into equation (7). That is, for a given bow speed V_B , as the spindle radius R_o goes up, the angular velocity ω goes down, cancelling the increased power we might expect by examining equation (7) in isolation. This is somewhat contrary to the common observation that smaller diameter spindles aid in faster ember formation. While this is mostly true (assuming spindles aren't so thin that structural integrity is compromised), the effect is actually due to the stronger concentration of heat energy on the face of the forming ember, as we will see in the next section.

Before moving on there are two other observations worth mentioning. First, we have all probably seen scouts and adults who've leaned on their spindles so hard that they've seized and stopped spinning. In the introduction to this article I mentioned that I would assume variable independence. Well, at least in the extreme, average bow speed V_B depends on the normal force F_N . Remember that the power expressed in equation (9) is actually coming from the firemaker him/herself! If the firemaker has sufficient strength and stamina to maintain bow speed, then by all means lean away and increase F_N as much as possible. For most of us though, it's probably best to lean on our spindles only to the point just before we are unable to sustain a healthy bow speed for a minute or so.

Lastly, from time to time you may encounter a bow drill spindle that has been carved into an hourglass shape. Does that help? Well, maybe. See Appendix D for details.

5. Ember Ignition

In this section I will develop a relationship for the lower bound Δt_{min} on the time required to ignite an ember. This lower bound will be for *initial* ember ignition only, without consideration of additional time a firemaker may allow a young ember to grow prior to transferring it to a tinder bundle. I will start by assuming that the heat generated by friction is uniformly distributed across the interface of the spindle and fireboard divot. I will also assume a common starting temperature (typically the ambient environmental temperature) for both the spindle and fireboard, and I must assume that the firemaker is experienced, uses good technique, and that the fireboard notch is initially filled with charcoal dust. I have no way to mathematically model and account for awkwardness, nor have I made any attempt to model the chemical-mechanical processes by which woods are charred and ground away to create charcoal dust.

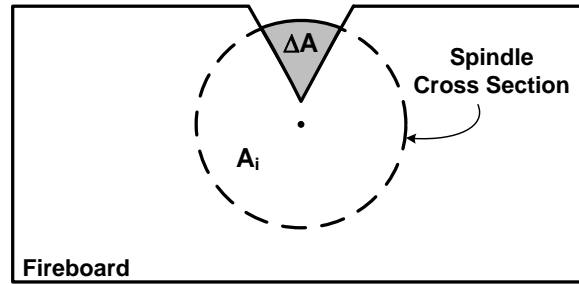


Figure 6: Initial ember ignition takes place where the charcoal dust directly contacts the heated spindle face.

Energy created by friction heats the charcoal dust up to its ignition temperature, at which time an ember begins to form at the top of the fireboard notch where the dust comes into direct contact with the heated spindle face. By inspection of Figure 6, the fraction of the friction generated heat W_E that is exposed to the forming ember is

$$W_E = W_F \frac{\Delta A}{A_i} = W_F \frac{\Delta A}{\pi(R_o^2 + h_o^2)} \quad [J], \quad (10)$$

where W_F is the total heat energy (or work) due to friction as expressed in equation (6), ΔA is the area (estimated or measured) of the spindle face exposed to the charcoal dust, $A_i = \pi(R_o^2 + h_o^2)$ is the area of the *spherical* spindle-divot interface, R_o is the spindle radius and h_o is the divot depth as shown in Figure 23 [12]. An example image of the ignition area of an actual fireboard notch is provided in Figure 7.

Next, the heat energy ΔQ required to raise a material by ΔT degrees is given by

$$\Delta Q = m C_p \Delta T \quad [J], \quad (11)$$

where m is the mass of the material being heated in grams [g], the change in temperature ΔT has units of degrees Celsius [°C] and C_p is the material's Specific Heat Capacity (or just Specific Heat) [13, 14, 15].



Figure 7: Example ignition area of a fireboard notch.

I will use specific heat values expressed in units of [J/g-°C] (there are others). Specific heat therefore represents the energy required to raise one gram of a material by one degree Celsius. That is, as C_p increases it takes more heat energy to increase the temperature of the material. (Thermal insulators generally have larger specific heats than thermal conductors, for example.) Most woods have specific heats in the range 2 (Oak) < C_p < 2.9 (Balsa). White pine has an average specific heat of 2.5 [J/g-°C], cast iron's specific heat is approximately 0.46 [J/g-°C] and, of particular interest to us, charcoal has a specific heat of about 1.0 [J/g-°C]. Future experiments to measure C_p for charcoal dusts created from a variety of common friction fire woods might be of interest to pursue.

In our case $\Delta Q = W_E$, the fraction of the friction created heat exposed to the face of the forming ember. Using equations (6) and (10) in equation (11) thus yields

$$\left(\frac{2}{3} \mu_k F_N R_o S_M(\rho) \theta\right) \left(\frac{\Delta A}{\pi(R_o^2 + h_o^2)}\right) = m C_p \Delta T , \quad (12)$$

where m is now the mass of charcoal dust required for initial ember ignition (typically small). Notice, though, that the cumulative angle of rotation θ can be expressed as

$$\theta = \omega \Delta t = \frac{V_B}{R_o} \Delta t \text{ [rad]}, \quad (13)$$

where Δt is the total time the spindle rotates at average angular velocity ω (either clockwise or counterclockwise). By inserting equation (13) into equation (12), rearranging terms and changing notation slightly we can find the relationship for Δt_{min} , the lower bound on the amount of time (i.e., the minimum time) it takes for initial ember ignition, under the conditions discussed at the start of this section. That is,

$$\Delta t_{min} = \Delta T \frac{3}{2} \frac{C_p}{\mu_k} \frac{m}{F_N} \frac{\pi(R_o^2 + h_o^2)}{\Delta A S_M(\rho)} \frac{1}{V_B} \text{ [s]} . \quad (14)$$

Equation (14) is the principle result of this article. It provides the lower bound on the time to ember ignition based upon assumptions stated at the beginning of this section, and the assorted variable values that will necessarily change according to the firemaker, kit and circumstances. In all cases, starting with an empty notch and using poor technique will result in a longer ignition time than Δt_{min} .

Despite the mathematical gymnastics required to arrive at equation (14), the result is simple, elegant and complete. All the variables interact in ways that are intuitively pleasing and in keeping with common experience. In particular, as alluded to in Section 4, notice that Δt_{min} decreases due to increased heat concentration as the spindle radius R_o , and thus the interface area $A_i = \pi(R_o^2 + h_o^2)$, decreases. Though not accounted for above, increased heat concentration as R_o decreases will no doubt also lead to faster wood charring and dust formation as well.

As a final thought for this section, notice that the interface area A_i , and the spherical moment factor $S_M(\rho)$ both depend on the spindle radius R_o . That is, they are not independent. In light of this fact I take a more nuanced look at equation (14) in Appendix E. However, I suggest you study Appendix E only after you've read through the rest of this article.

6. Experimental Verification

In order to test the validity of equation (14) I set up some experiments in my basement one evening. Out of a sense of nostalgia I decided to use my very first Slippery Elm (a.k.a. Red Elm) bow drill set – the one I made at Camp Ransburg in 2016. Although I am now fairly experienced with the bow drill, I hadn't used this particular kit in a long time and so I thought some practice was in order. I ended up making three embers from scratch (i.e., I did not initially fill the notch with charcoal dust), which I then quickly put out and weighed. The average mass of the piles of dust that formed these three embers was only 0.8 grams. Of course, most of the dust does not come into close contact with the base of the spindle at the top of the fireboard notch. No more than a fraction of the dust pile is actually required for *initial* ignition and so I decided to set $\mathbf{m} = \mathbf{0.1 [g]}$ in equation (14).

Next, I placed the fireboard on my digital bathroom scale and leaned on it just as I do when bowing up an ember. So that I would not be prone to influencing the results, I asked my daughter to read the scale and record the measurements for me. We repeated this measurement four times and found that I was applying an average normal/downward force of 13.5 pounds. Converting to SI units, I will use a value of $\mathbf{F_N = 60 [N]}$ in later calculations. This is consistent with prior measurements made by me and others [16, 17, 18].



Figure 8: A freshly burned-in Slippery Elm spindle.

I then trimmed the sides of my spindle a bit, after which I burned-in and notched a new, freshly carved divot in my fireboard. The charred spindle tip is shown in Figure 8. To create the condition assumed for equation (14) to apply, I then filled the notch with dust I had collected earlier in the evening and asked my teenage children to help record a video of me bowing up an ember. For your inspection, this video can be accessed through the following link [19]

Data Video Link: <https://youtu.be/K0CPU6TCYZw>

After carefully inspecting this video I made the following observations. First, I counted 35 full (i.e., forward *and* backward) bow strokes over a period of 21 seconds (I started counting at 1:54 and concluded at 2:15). By observing how/where I was holding and manipulating my bow, I also estimated that my average bow stroke length (forward *or* backward) was 22 inches – see Figure 9. This results in an average bow speed of

$$V_B = \frac{2 \cdot 22 \cdot 35}{21} = 73 \frac{1}{3} \text{ [in/sec]} .$$

Converting to SI units gives us $V_B = 1.86 \text{ [m/s]}$. Recall that as an average bow speed, V_B takes into account all the starting, stopping and direction reversals, etc., observed in the data video.



Figure 9: I generally prefer longer bows. From the video referenced above, I estimated that full bow strokes were about 22 inches long on average.

Upon further inspection of the video I noted that I bowed for a total time of 25 seconds (starting at 1:53 and stop at 2:18). However, an experienced firemaker can typically tell that an ember has ignited when smoke is seen emanating from the dust in front of, and noticeably distant from, where the spindle and fireboard divot are tangent to one another in the area of the fireboard notch. I made this observation shortly before I stopped bowing. My best estimate of the time till initial ember formation is therefore in the range of $23 < \Delta t < 24 \text{ [s]}$. You'll also notice in the video that it took some time for the new ember to eventually grow to appreciable size. Recall, though, that it's the time till *initial* ignition that is of interest here.

After disposing of the ember I inspected the spindle and fireboard and made some more measurements. As seen in the images of Figure 10, the charred spindle/divot diameter is

approximately one inch, yielding a measured spindle radius of $R_o = 0.5$ [in.]. The average diameter of the spindle where the bow string was attached was also very nearly one inch. Next, by examination of the charred region of the spindle using my digital calipers, the depth of the divot was determined to be $h_o = 0.166$ [in.]. Next, the triangular ignition area of my fireboard notch was carefully measured to yield a base length of 0.309 [in.] and a depth of 0.407 [in.], yielding a value of $\Delta A = (\text{base} \times \text{depth})/2 = 0.0629$ [in.²].

Others have previously done experiments to determine the temperature at which fire by friction charcoal dust ignites. Most measurements have yielded results in the range of 650-800 [°F], with the most reliable estimates on the order of 700 [°F] [20, 21]. The thermometer in my basement read 63 [°F] during the time of my experiments, meaning that I needed to create friction heat sufficient enough to raise the dust by $\Delta T = (700-63)/1.8 = 354$ [°C].

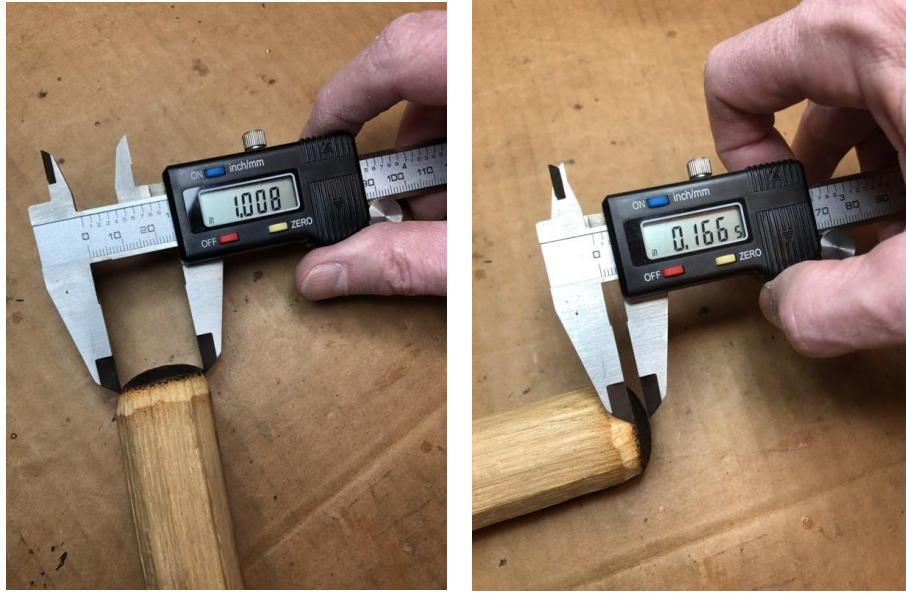


Figure 10: Spindle diameter and divot depth measurements.

Next we need to determine the value of the spherical moment factor $S_M(\rho)$ applicable to the experiment. To make the calculation, we first need to know the radius of curvature R_c of the very nearly spherical spindle-divot interface. This can be determined from the relationship for the area A_i of a spherical cap expressed as [12]

$$A_i = \pi(R_o^2 + h_o^2) = 2\pi R_c h_o \text{ [in.}^2\text{]}. \quad (15)$$

Solving for R_c we find

$$R_c = \frac{R_o^2 + h_o^2}{2 h_o} \text{ [in.]} \quad (16)$$

Using the previously stated measured values for R_o and h_o , from equation (16) we find that $R_c = 0.836$ [in.]. This in turn yields a value of $\rho = R_c/R_o = 1.672$, after which equation (5) gives us a spherical moment factor for this experiment of $S_M(\rho) = 1.134$, shown by the red dot in Figure 4. The nearly spherical shape of the spindle is confirmed in Figure 11.



Figure 11: The spindle-divot interface is very nearly spherical in shape.

In order to use equation (14) to calculate the expected minimum time for initial ember ignition according to the parameters of my experiment, as stated in Sections 2 and 5 I will assume values of $\mu_k = 0.25$ and $C_p = 1.0 \text{ [J/g-}^\circ\text{C]}$ for the kinetic coefficient of friction and specific heat, respectively. Inserting these values, and the other appropriate **bold** faced values of this section into equation (14) then yields an expected minimum time to ignition of $\Delta t_{min} = 23.27 \text{ [s]}$. This is remarkably close to my observed estimate of 23-24 [s]. With some admitted uncertainty in my measurements and also in the values used for μ_k , C_p and the temperature required for ember ignition (though in all cases reasonable best estimates were used), where additional experimentation might be of interest, I believe the results of Section 5, equation (14) in particular, have been confirmed. Only the test of time, with further analysis and more careful experimentation, will confirm this with certainty.



Figure 12: Twenty-one Watts is enough to power five night light bulbs.

Finally, I was curious to see how much power I was generating to create my ember. Using the appropriate values from this section in equation (9) I calculated just a bit over 21 [W]. That's enough to power five of the little 4W night light bulbs shown in Figure 12. It doesn't seem like much, but most would agree that driving a bow drill can on occasion be a tiring experience.

7. Pump Drill Modifications

Before concluding I want to spend some time considering the pump drill method of fire by friction and what might be required for equation (14), which expresses the lower bound Δt_{min} on the time required for initial ember ignition, to apply. It turns out that we need only make modifications to the normal force F_N and the “effective” bow speed V_B . Beginning with the normal force, for the pump drill we can use

$$F_N = \frac{1}{2}(F_P + m_{pd} 9.81) \text{ [N]}, \quad (17)$$

where m_{pd} is the mass of the pump drill apparatus in [kg] and F_P is the total force applied during the downward pump cycle. For equation (17) I am assuming a 50% duty cycle between the up/down power and spin-up strokes, in keeping with observations I’ve made when using my own pump drills [22]. The effective normal pump drill force F_N is thus the simple average of F_P and the weight (mass times acceleration due to gravity) of the pump drill itself. That is, on the spin-up portion of each cycle, only the weight of the pump drill apparatus causes a downward force on the spindle/fireboard interface.

For us to determine an effective bow speed V_{Beff} for the pump drill we need to recall that it is the cyclic pumping action, not bowing, that causes spindle rotation. To proceed I will need to define two new variables, N_R and P_S . The first variable, N_R , is the number of shaft rotations per up *or* down stroke (i.e., during one half cycle) on the pump bar. This is probably best measured by hand winding the pump bar on the pump drill shaft. Note that it is possible for N_R to be fractional, so careful measurements are in order. Note also that N_R is unitless. As an example, for my own pump drills N_R is ~ 3 .

The next new variable, P_S , is the time averaged pump rate (i.e., it accounts for all pump bar starts, stops and direction reversals, etc.). The units of P_S is [1/s] and a single pump period is taken to mean a full up/down power stroke *and* spin-up cycle. This parameter will be highly dependent on the pump drill itself as well as the firemaker’s skill, strength and stamina. For my largest pump drill, I have measured a value of $P_S = 1.86$ [1/s] with the aid of video [22].

The number of spindle rotations per second R_S can now be written as

$$R_S = 2 P_S N_R \text{ [1/s]}. \quad (18)$$

The angular velocity of the spindle is then $\omega = 2\pi R_S = 4\pi P_S N_R$ [1/s]. Using this result in equation (8) and rearranging we find that the effective bow speed V_{Beff} is

$$V_{Beff} = 4\pi R_o P_S N_R \text{ [m/s]}. \quad (19)$$

Now we merely need to use the results of equations (17) and (19) in equation (14) to determine the lower bound $\Delta t_{min-pump}$ on the time till initial ember ignition for the pump drill. Specifically,

$$\Delta t_{min-pump} = \Delta T \frac{3}{4\pi} \frac{C_P}{\mu_K} \frac{m}{(F_P + m_{pd} 9.81)} \frac{\pi(R_o^2 + h_o^2)}{\Delta A S_M(\rho)} \frac{1}{R_o P_S N_R} \text{ [s]}. \quad (20)$$

Aside from my estimates of P_S , N_R and the 50% up/down duty cycle mentioned above I have not yet done further work to experimentally verify equation (20). Perhaps that’s something I’ll pursue that when the weather is warmer. You might give it a try as well.

To conclude this section I should point out that while the pump drill may for many be easier to learn than the bow drill, my personal observation is that it is slower to form embers and less efficient overall. The pump drill is disadvantaged by the reduced downward force during the spin-up portion of the pump cycle. To reduce this effect it helps to have a heavy pump drill apparatus. In particular it helps to have a heavy flywheel. It also helps to use a flywheel with a large moment of inertia – i.e., one for which the bulk of the flywheel mass is positioned far from the axis of rotation. I like to use cast iron caster wheels in my pump drills [22]. A high moment of inertial flywheel will also help on the spin-up cycle by preserving rotational momentum, thereby increasing both pump speed and the effective bow speed. Note that while these effects are implied, they are not explicitly accounted for in equation (20).

8. Conclusion

So, what have we learned? From a practical firemaking perspective maybe we haven't learned all that much. The main result of this article is equation (14) (rewritten as equation (E6) in Appendix E), and that doesn't tell us a great deal beyond what many of us already know from experience – i.e., you can make faster embers if you press on the spindle harder, bow faster, etc. Perhaps, though, you might find it satisfying, as I do, that the physical principles of fire by friction can be so well described mathematically, with all the variables coming together in such an intuitive way. I was also quite surprised to learn that the speed of ember formation is so strongly influenced by the shape of the spindle and fireboard divot interface. Have you read Appendix E? If not, please go read it. There I demonstrate that by carefully carving our spindles to be hemispherical in shape we can potentially reduce the minimum time to ember ignition by an extraordinary 15%. Wow!

If I get the chance there are a few things I'd like to investigate further. Perhaps we could collaborate if you are interested. In particular, I'd like to determine better values for the coefficients of kinetic friction μ_k for charred woods commonly used in fire by friction kits. I'd also like to further investigate the specific heats C_p and ignition temperatures of charcoal dusts created from these woods. It's probably beyond my own capabilities, but some really ambitious soul might look into the effects of heat transfer at the spindle-fireboard interface. I didn't account for any differences in thermal diffusivity for wood and charcoal dust, for example. I just assumed friction generated heat was uniformly distributed across the spindle-fireboard interface. A more careful analysis of the heat transfer characteristics might also yield a better estimate of the minimum dust mass m required for ignition. Someone might even take on the challenge of modeling the chemical-mechanical processes by which woods are charred, ground away and collected in the fireboard notch. Lastly, it might be fun to set up a mechanically controlled system what would allow the normal force F_N and spindle angular velocity ω to be precisely fixed. This would allow equation (14) to be tested without the uncertain effects of human imprecision and error.

Till then, keep practicing and be mindful of the variables you can control to make faster embers. Use a thin fireboard for faster dust accumulation if you can't start with a filled notch. Use a skinny spindle, as long as structural integrity isn't compromised. Carve a hemispherical tip onto your spindle, for up to 15% faster ember formation than with a blunt spindle. Press down as hard as you can without seizing the spindle. Eat your Wheaties. Be in good shape. Breathe! And bow like mad using full strokes!

That's it. If you've made it to the end, thank you for the time you've invested. I hope I got it right and that you've learned some things of interest and perhaps valuable to your continued firemaking adventures. If you have questions or suggestions for improvement, I'd love to hear from you.



Figure 13: My first friction fire. Firecrafter shelter, Ransburg Scout Reservation, June, 2016.

Best Wishes,

Bradley D. Duncan XXX
Assistant Scoutmaster, Troop 516, Centerville, OH
Advisor, Miami Shawnee Ember of Firecrafter

© Copyright, 2021, Bradley D. Duncan, Ph.D.

This article is the sole intellectual property of the author and was produced without sponsorship or support. It may be downloaded and distributed free of charge for private use, and may be used and referenced by others with proper attribution and credit to the author. No permission is required except for commercial use, distribution and/or reproduction.

9. References

The Firecrafter Organization:

1) <https://firecrafter38.wildapricot.org/>

Static and Kinetic Friction:

2) <http://hyperphysics.phy-astr.gsu.edu/hbase/frict2.html>

3) <https://physics.info/friction/>

Coefficients of Friction:

4) <https://www.physlink.com/reference/frictioncoefficients.cfm>

5) https://www.engineersedge.com/coeffients_of_friction.htm

Bearing Pressure

6) https://handwiki.org/wiki/Physics:Bearing_pressure

Disc Friction:

7) http://mechanicsmap.psu.edu/websites/6_friction/disc_friction/discfriction.html

Rotational Work and Kinetic Energy:

8) <https://www.dummies.com/education/science/physics/how-to-calculate-rotational-work/>

9) <https://www.youtube.com/watch?v=-DPthKuQGyQ>

10) <http://hyperphysics.phy-astr.gsu.edu/hbase/rke.html>

11) http://spiff.rit.edu/classes/phys211_spr1999/lectures/rotke/rotke_all.html

Area of a Spherical Cap or Divot

12) <http://www.ambrsoft.com/TrigoCalc/Sphere/Cap/SphereCap.htm#cap>

Specific Heat and Values for Various Solids:

13) https://en.wikipedia.org/wiki/Specific_heat_capacity

14) https://www.youtube.com/watch?v=Q63QPec_1bk

15) https://www.engineeringtoolbox.com/specific-heat-solids-d_154.html

Hand Drill and Bow Drill Force Experiments:

16) <https://www.youtube.com/watch?v=yV0FDebQzCk>

17) <https://www.youtube.com/watch?v=7bdfz6WluRs>

18) <https://www.youtube.com/watch?v=SycYjJKSA3s>

Experimental Data Video:

19) <https://youtu.be/K0CPU6TCYZw>

Charcoal Dust Ignition Temperatures:

20) https://www.primitiveways.com/fire_Baugh.html

21) https://www.primitiveways.com/fire_Baugh2.html

Pump Drill Fire by Friction:

22) <https://www.youtube.com/watch?v=BgAiIEEsXFc>

Appendix A: What's a Newton of Force?

From Newton's second law we know that force F equals mass m times acceleration a , or

$$F = ma [N], \quad (A1)$$

where mass is expressed in kilograms [kg] and acceleration has units of meters per second-squared [m/s²]. If we assume we have a mass acted upon only by the acceleration due to gravity, 9.81 [m/s²], we might ask ourselves what mass m_{1N} is required to create a downward gravitational force of only 1 [N]. Solving [A1] for m_{1N} easily yields

$$m_{1N} = \frac{1}{9.81} [kg] = 0.102 \text{ kg} = 102g.$$

As I was preparing to write this article, I went around my house one afternoon and weighed a variety of objects with my digital kitchen scale. Interestingly, I discovered a bag of medium sized Honey Crisp apples whose mass averaged just a bit over 200 grams. So, on average, if you hold a medium sized apple in your hand, it exerts an approximately 2N downward force against you. Likewise, due to Newton's third law, assuming you hold the apple stationary you are also exerting an upward force of 2N on it.

Cool!



Figure 1A: An approximately two Newton apple!

Appendix B: Effect of the Fireboard Notch on Net Moment

What happens to the net moment due to friction if we exclude a wedge shaped notch from our calculations where charcoal dust collects and the ember ultimately ignites? To address this question most easily I will first assume a planar spindle-fireboard interface, for which $R_c \gg R_o$ in Figure 3.

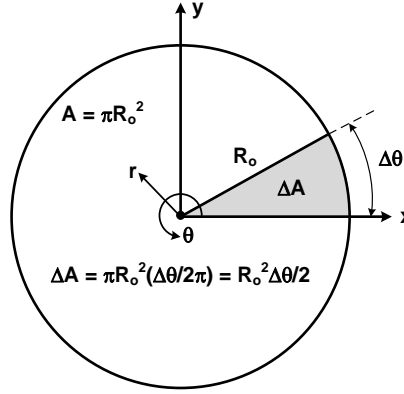


Figure 1B: Geometry of a planar spindle-fireboard interface from which a notch of area ΔA has been removed.

The geometry of the problem in planar polar coordinates is shown in Figure 1B. The radial variable is r , the azimuth angle is θ and the spindle/divot radius is R_o . The cross sectional area of the spindle and divot is $A = \pi R_o^2$, and the wedge shaped notch, shaded gray, has an area $\Delta A = R_o^2 \Delta\theta/2$, where $\Delta\theta$ is the angular extent of the notch. The net moment at the flat/planar interface is then expressed as

$$M_f = \int_0^{R_o} \int_{\Delta\theta}^{2\pi} f(r, \theta) dA \text{ [N-m]}, \quad (\text{B1})$$

where the incremental moment per unit area $f(r, \theta) = \mu_k P r$ [N/m], and where in polar coordinates the differential area $dA = r dr d\theta$ [m²]. The pressure P is in turn given by

$$P = \frac{F_N}{A - \Delta A} = \frac{2F_N}{R_o^2 (2\pi - \Delta\theta)} \text{ [N/m}^2\text{]}. \quad (\text{B2})$$

If we insert $f(r, \theta)$ and equation (B2) into equation (B1), then integrate and simplify we find

$$\begin{aligned} M_f &= \mu_k \frac{2F_N}{R_o^2 (2\pi - \Delta\theta)} \int_0^{R_o} \int_{\Delta\theta}^{2\pi} r^2 dr d\theta \text{ [N-m]} \\ M_f &= \mu_k \frac{2F_N}{R_o^2 (2\pi - \Delta\theta)} (2\pi - \Delta\theta) \int_0^{R_o} r^2 dr \text{ [N-m]} \\ M_f &= \mu_k \frac{2F_N R_o^3}{R_o^2 \cdot 3} = \frac{2}{3} \mu_k F_N R_o \text{ [N-m]}. \end{aligned} \quad (\text{B3})$$

Notice that the result of equation (B3) is identical to the result of equation (4) if the spherical moment factor $S_M(\rho)$ is set to unity (i.e., when $R_c \gg R_o$). We therefore conclude that consideration of the notch does not affect the calculation of net moment due to friction. As mentioned earlier, the increased pressure when the notch is removed is integrated over a correspondingly smaller area. The effects then cancel and the net moment results are unaffected.

Appendix C: “Radians” – a Unitless Unit

An often confusing and unexpected fact is that angular measurements are actually unitless. We typically express angles in degrees, radians and even gradians. These are, however, unitless dimensions that merely serve to tell us how finely we can divide up our circles. To demonstrate we will consider the “radian.”

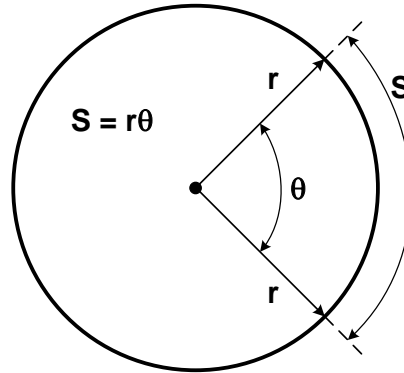


Figure 1C: The basic geometry of a circle.

Recall from an introductory course in Geometry that the arc length S shown in Figure 1C is the physical distance between two points along a section of a circle. The arc length is calculated as follows

$$S = r \theta \text{ [m] ,} \quad (\text{C1})$$

where r is the radius of the circle and θ is the angle subtending S . Since both arc length S and the radius r have units of meters [m], the angle θ *must* be unitless. In other words, θ is just a factor that tells us how long the arc length S is in relation to the circle’s radius.

Rearranging equation (C1) we find

$$\theta = \frac{S}{r} \text{ [rad] .} \quad (\text{C2})$$

Notice, though, that $[\text{rad}] = [\text{m}/\text{m}] = 1$, meaning that the radian is indeed a unitless unit. Moreover, it’s important to note that angular velocity ω and angular acceleration α also have units as follows

$$[\omega] = \frac{\text{radians}}{\text{second}} = \frac{1}{\text{s}} , \quad (\text{C3})$$

and

$$[\alpha] = \frac{\text{radians}}{(\text{second})^2} = \frac{1}{\text{s}^2} , \quad (\text{C4})$$

where the notation [variable] means “units of” the variable, and [second] = [s].

Appendix D: Effect of Hourglass Shaped Spindles

On occasion you might encounter a firemaker who likes to carve his/her bow drill spindle into an hourglass shape. You might wonder if this makes any difference. In some cases it might, as we can determine by examining Figure 1D, below.

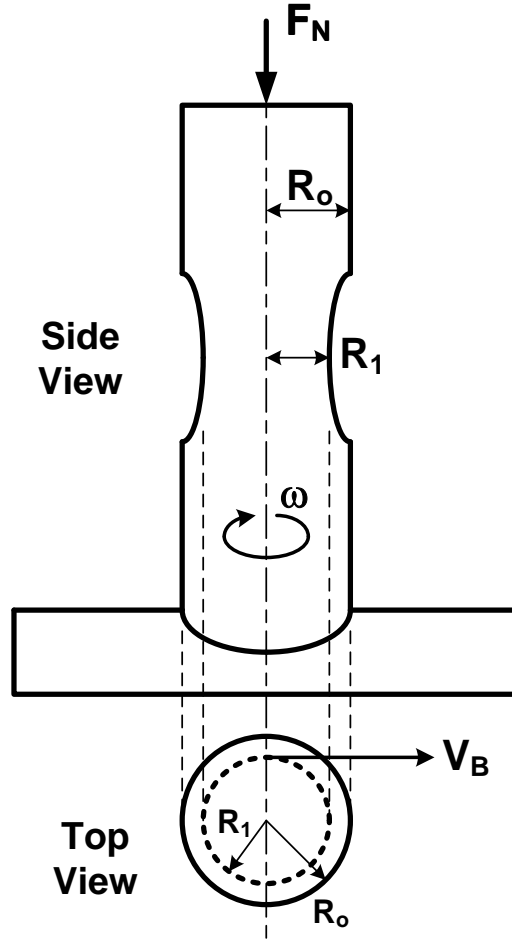


Figure 1D: An hourglass shaped spindle may aid in faster ember formation.

If we attach our bow string to the middle of the spindle where the radius is R_1 , then the angular velocity of the spindle becomes $\omega = V_B/R_1$, where V_B is the time averaged bow speed. Inserting the new value for angular velocity into equation (7) results in the following relationship for friction induced power generation (i.e., energy released per unit time)

$$P_F = \frac{2}{3} \mu_k F_N \frac{R_o}{R_1} S_M(\rho) V_B \text{ [W]}, \quad (\text{D1})$$

where as before, the nominal radius of the spindle is R_o . Since $R_1 < R_o$ it therefore appears that an hourglass shaped spindle does serve to increase power generation for a given bow speed V_B . However, assuming structural integrity of the spindle is not compromised, it would probably be better to carve the spindle from top-to-bottom with the smaller radius R_1 from the start. As discussed in Section 5, a thinner spindle will concentrate the friction induced heat energy into a smaller area, thereby aiding in more rapid ember formation.

What about the more common situation shown in Figure 2D? Here we see a uniform radius spindle that does not fully engage the fireboard divot. This situation might arise when a new divot has recently been carved into the fireboard and freshly burned-in. It might also arise when a spindle is trimmed to avoid side friction in a deeper divot. Regardless, the radius R_1 of the spindle where the bow string is attached is larger than the radius R_o of the spindle where it actually engages the fireboard. Just as above, the angular velocity of the spindle is $\omega = V_B/R_1$, where V_B is the time averaged bow speed, and the relationship for friction induced power generation in equation (D1) remains unchanged. In this case, though, $R_1 > R_o$ and power generation is reduced.

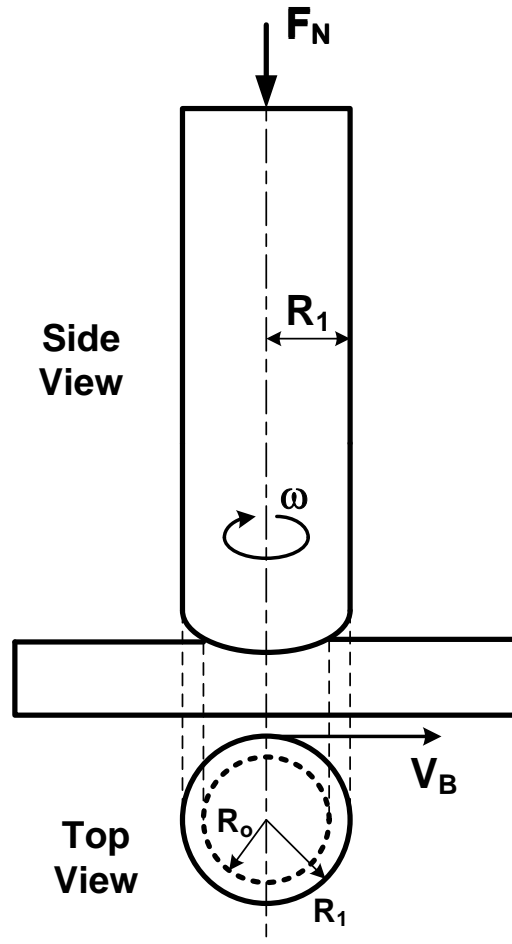


Figure 2D: Power generation is reduced when a uniform diameter spindle does not fully engage the fireboard divot.

As a general observation, note that throughout this article if the radius R_1 of the spindle where the bow string is attached is *different* from the radius R_o of the spindle where it engages the fireboard, the average bow speed V_B should be multiplied by R_o/R_1 . Compare, for example, equations (9) and (D1).

Appendix E: Another Look at the Relationship for Minimum Time to Ignition Δt_{min}

As I mentioned briefly at the end of Section 5, the spindle-fireboard interface area A_i , and the spherical moment factor $S_M(\rho)$ both depend on the spindle radius R_o , meaning that they are not independent. It's actually a bit more involved than that. Notice, for example, that in Figure 3 I have tacitly assumed that the spherically curved shape extends over the full extent of the spindle endface. Therefore, as the radius of curvature R_c decreases toward the spindle radius R_o , the divot depth h_o must increase. Likewise, as R_c grows large, the divot depth approaches zero. In the extreme limits we have

$$\text{as } R_c \rightarrow R_o, h_o \rightarrow R_o, \rho \rightarrow 1, S_M(\rho) \rightarrow 3\pi/4 \text{ and } A_i = \pi(R_o^2 + h_o^2) \rightarrow 2\pi R_o^2$$

$$\text{and, as } R_c \rightarrow \infty, h_o \rightarrow 0, \rho \rightarrow \infty, S_M(\rho) \rightarrow 1 \text{ and } A_i \rightarrow \pi R_o^2 .$$

We can also see the coupling of these variables in the alternative relationships for A_i given in equation (15), which I repeat here

$$A_i = \pi(R_o^2 + h_o^2) = 2\pi R_c h_o \text{ [in.}^2\text{]} . \quad (\text{E1})$$

Due to these variables interactions it is possible to express equation (14) in a somewhat more compact form that will provide an interesting insight into the effect of spindle/divot shape on the expected minimum time required for ember formation. To begin, I repeat equation (14) here

$$\Delta t_{min} = \Delta T \frac{3}{2} \frac{c_p}{\mu_k} \frac{m}{F_N} \frac{\pi(R_o^2 + h_o^2)}{\Delta A S_M(\rho)} \frac{1}{V_B} \text{ [s]} . \quad (\text{E2})$$

Then, after a great deal of mathematical gymnastics (i.e., mostly algebra, with a little trigonometry), the factors of equation (E2) that I have highlighted in red can be written as

$$\frac{\pi(R_o^2 + h_o^2)}{S_M(\rho)} = \frac{2\pi R_c h_o}{S_M(\rho)} = \dots = (\pi R_o^2) S_M^*(\rho) , \quad (\text{E3})$$

where

$$S_M^*(\rho) = \frac{4}{3} \frac{1 - \sqrt{1 - \left(\frac{1}{\rho}\right)^2}}{\rho \sin^{-1}\left(\frac{1}{\rho}\right) - \sqrt{1 - \left(\frac{1}{\rho}\right)^2}} . \quad (\text{E4})$$

$S_M^*(\rho)$ is now an aggregate spherical shape factor where, as before, $\rho = R_c/R_o$. In deriving equations (E3) and (E4) I used a variety of mathematical steps similar to those employed in earlier sections. I also used the fact that (see Figure 3)

$$h_o = R_c - R_c \cos(\varphi_o) = R_c \left(1 - \cos \left(\sin^{-1} \left(\frac{R_o}{R_c} \right) \right) \right) = R_c \left(1 - \sqrt{1 - \left(\frac{1}{\rho} \right)^2} \right) . \quad (\text{E5})$$

We can then rewrite equation (E2) as

$$\Delta t_{min} = \Delta T \frac{3}{2} \frac{c_p}{\mu_k} \frac{m}{F_N} \frac{1}{V_B} \frac{\pi R_o^2}{\Delta A} S_M^*(\rho) \text{ [s]} . \quad (\text{E6})$$

As with the spherical moment factor discussed in Section 3, at first glance the new aggregate spherical shape factor appears daunting. It too, however, is very well behaved as shown in Figure 1E.

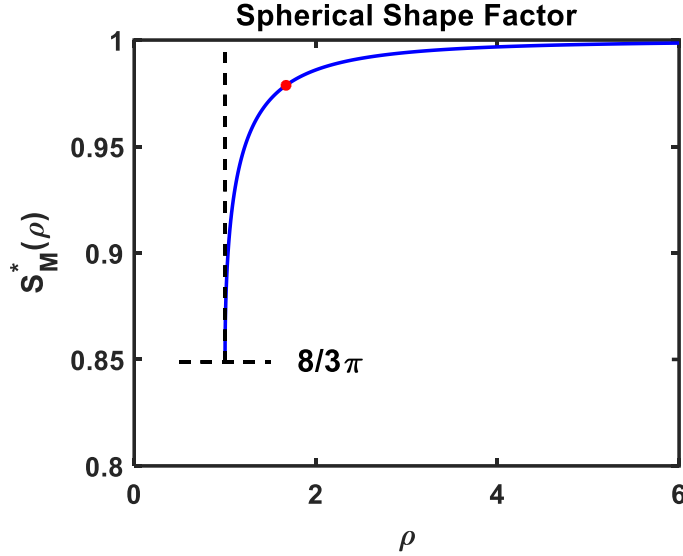


Figure 1E: The aggregate spherical shape factor approaches unity for a nearly flat spindle-fireboard interface surface, and approaches $8/3\pi$ as the interface becomes increasingly hemispherical. The red dot represents the value realized in the experiment discussed in Section 6.

Notice that for an increasingly blunt spindle endface, as the radius of curvature R_c increases the parameter ρ also increases and $S_M^*(\rho)$ approaches unity. However, for a highly hemispherical spindle-fireboard interface, for which $R_c = R_o$ or $\rho = 1$, the shape factor approaches $8/3\pi = \sim 0.8488$. In other words, by carefully carving our spindles to have hemispherical shapes we can potentially reduce the minimum time to ember ignition by 15%. This is extraordinary! Rarely does the physical world offer us the opportunity to increase efficiencies so dramatically by such easily controlled means.

Finally, as a matter of completeness, using equations (E3) and (E4) the lower bound $\Delta t_{min-pump}$ on the time till initial ember ignition for the pump drill can be rewritten as

$$\Delta t_{min-pump} = \Delta T \frac{3}{4\pi} \frac{C_p}{\mu_k} \frac{m}{(F_P + m_{pd} 9.81)} \frac{\pi R_o^2}{\Delta A} \frac{S_M^*(\rho)}{R_o P_S N_R} \text{ [s] } , \quad (E7)$$

where all the variables in equation (E7) remain as they have been defined in preceding sections.